ARTICLE

Catalytically Assisted Tip Growth Mechanism for Single-Wall Carbon Nanotubes

J.-C. Charlier,[†,*] H. Amara,[†,‡] and Ph. Lambin[‡]

[†]Unité de Physico-Chimie et de Physique des Matériaux (PCPM-CERMIN), Université Catholique de Louvain, Place Croix du Sud, 1 (Boltzmann), B-1348 Louvain-la-Neuve, Belgium, and [‡]Laboratoire de Physique du Solide, Facultés Universitaires Notre-Dame de la Paix, 61 Rue de Bruxelles, 5000 Namur, Belgium

ABSTRACT The catalytic growth of single-wall carbon nanotubes is investigated at the nanotube tip using first-principles molecular dynamics and *tight-binding* Monte Carlo simulations. At experimental temperatures (~1500 K), the catalytic atom is found to incorporate into the carbon network instead of scooting around the open edge. Consequently, the open end of SWNTs closes spontaneously into a graphitic dome, suggesting a closed-end mechanism for the catalytic growth. At 1500 K, the cobalt–carbon chemical bonds keep breaking and reforming, providing a direct incorporation process for additional carbon, necessary for growth. The catalytic action of Co atoms is also found to play a key role in the reconstruction of the nanotube tip after carbon incorporation, by annealing defects. The present closed-end tip growth mechanism may coexist with the usual root growth mechanism.

KEYWORDS: carbon nanotubes · catalytic growth · growth mechanisms at the atomic scale · ab initio calculations · quantum molecular dynamics · tight-binding Monte-Carlo simulations

In contrast with multi-wall nanotubes (MWNTs),[1] the formation of single-wall carbon nanotubes (SWNTs) is triggered by enriching the graphite source material with a pure transition metal catalyst (Co, Ni, Fe, Y, ...), or a mixture thereof.[2–6] Consequently, SWNTs are synthesized through the interaction of metal catalyst nanoparticles with carbon or hydrocarbon vapor at relatively high temperature. While the uncatalyzed growth of MWNTs has been rationalized,[7–9] the exact role played by the metal atoms in determining the growth of SWNTs remains controversial. In chemical vapor deposition (CVD) techniques, the hydrocarbon molecules dissociate at the interface between catalyst and vapor, and carbon atoms precipitate into a graphite trail in the shape of a nanotube. Just how the nanotube forms is still a debated issue. On the basis of experimental observations, it is commonly accepted that different scenarios should apply, depending on the size of the catalytic particle. When a large metal–carbide particle of a few tens of nanometers is present, the growth of SWNTs is believed to proceed *via* solvation of carbon vapor into the metal cluster, followed by segregation and precipitation of carbon excess in the form of a large number of SWNTs growing from the particle surface.[6,10,11] When the catalytic particle is smaller in diameter (just a few nanometers), it is frequently found trapped in the tip of SWNTs, and the diameter of the SWNTs is directly related to the particle size.[12–14] Consequently, the catalyst particle might stay at the growing end of the nanotube (tip growth),[12–14] or it might sit at the starting end (root growth),[6,10,11] both processes being analogous to what is observed *in situ* for the growth of carbon nanofibers.[15]

To go beyond phenomenological approaches, several theoretical groups have investigated the early stages of SWNT growth at the atomic level using different simulation techniques with varying accuracies, ranging from classical molecular dynamics[16,17] to *tight-binding* models[18] and finally to quantum molecular dynamics.[6,19–21] Most of these simulations support a root growth mechanism whereby carbon atoms are incorporated into the tube base by a diffusion–segregation process.[6]

The tip growth has also been investigated with a catalytic metal particle reduced to a few atoms at the open end of a nanotube. Its role consists in preventing the tube closure by scooting around and annealing defects, stabilizing the reactive dangling bonds, and allowing the incorporation of new carbon species from the gas phase.[4,22–24] All these calculations, suggesting an open-end tip growth mechanism, are based on static calculations. The aim of the present article is to provide insight at the atomic scale toward a better understanding of the SWNT formation mecha-nism, using dynamical effects that are

Ⓦ This paper contains enhanced objects available on the Internet at http://pubs.acs.org/journals/ancac3.

*Address corrspondence to jean-christophe.charlier@uclouvain.be.

Received for review May 30, 2007 and accepted September 24, 2007.

Published online October 31, 2007.
10.1021/nn700049q CCC: $37.00

© 2007 American Chemical Society

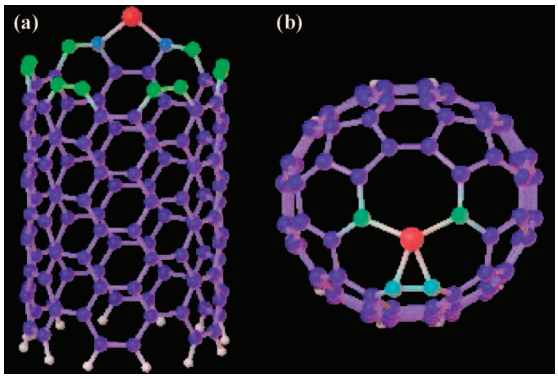

Figure 1. Spontaneous closure of a (6,6) armchair SWNT. The model contains 120 carbon atoms (blue and green spheres), 1 cobalt atom (big red sphere), and 10 hydrogen atoms (small white spheres at the bottom). Blue and green spheres represent carbon coordination of 3 and 2, respectively. Coordinations between 2 (green) and 3 (blue) are represented by the intermediate color palette. The hydrogen atoms and the neighboring bottom ring of carbons were kept fixed during the simulation. (a) Side view of the open-end starting configuration at 0 K, with 10 two-coordinated carbon atoms at the top edge and a Co atom forming a pentagon with four other carbons of the "armchair" edge (ground-state minimum). (b) Top view of the closed-end configuration after 12 ps at 1500 K and a quench to 0 K. The tip atomic structure is symmetric and composed of 6 pentagons, 12 hexagons, 1 heptagon, and 1 triangle.

Ⓦ A Quicktime movie (movie 1) showing a quantum molecular dynamics simulation of the spontaneous closure of a (6,6) armchair SWNT at 1500–2000 K is available.

Ⓦ A Quicktime movie (movie 2) showing a quantum molecular dynamics simulation of the incorporation of an additional carbon atom from the vapor phase into the catalyzed closed-end tip of a (6,6) armchair SWNT at ~2000 K is also available.

found crucial to unravel the atomic behavior of the metal catalysts when assisting growth.

RESULTS AND DISCUSSION

The dynamical interaction between Co catalyst at the tip of a growing nanotube and additional C atoms that are present is explored by allowing the system to evolve free of constraints at the experimental temperature, using quantum (*ab initio*) molecular dynamic (QMD) simulations (see Methods). When the tube is open-ended, the metal catalyst atom helps the open end of the SWNT to close spontaneously into a graphitic dome, suggesting a closed-end growth mechanism, in conflict with the scooting mechanism. The cobalt–carbon chemical bonds, enhancing the reactivity of the tip and providing the necessary pathway for incorporation of carbon atoms, support a model of growth by chemisorption from the vapor phase. The metal catalyst is also found to play a key role in the reconstruction of the nanotube tip during growth.

Following the existing model adopted in refs 4 and 21, we start with a (6,6) "armchair" nanotube section (0.8 nm in diameter, see Figure 1a) terminated on one side by an open end that contains one cobalt atom and on the other side by hydrogen atoms that passivate dangling bonds in order to mimic a semi-infinite system. During the course of the QMD simulations, the open end of the (6,6) single-wall tube closes into a structure with no residual dangling bonds (Figure 1b). The Co atom always tries to maximize the number of bonds with two-coordinated carbon atoms. This tendency had also been put forward in *tight-binding* calculations, where the importance of strong C–metal interactions is underlined.[18] This explains why, starting from the open edge (where Co is two-coordinated), the metallic atom tends to reach the center of the open end of the SWNT, thus initiating dome closure. The catalytic atom is not mobile, in the sense that it does not scoot along the open edge of the tube and does not anneal pentagons before being incorporated in the growing structure as previously suggested.[4,23] This closed-end topology, where Co is four-coordinated, is more stable than the initial open-end structure by ~21.2 eV when quenched to 0 K (Figure 1b).

During 9 ps of QMD simulation at 1500–2000 K, the metal atom moves frequently, thus creating and annihilating covalent bonds with carbon neighbors at the nanotube tip apex (see movie 1 in the electronic version of this article). At this temperature, the bond topology of the nanotube edge strongly fluctuates in close correlation with the metal atomic motion. Although the Co–C bonds are continuously breaking and re-forming, the catalyst atom stays always incorporated in the graphitic network, being sometimes coordinated with six carbons. Further, and even though the Co remains close to the tip apex, C–C bonds located a few atoms away from the catalytic atom are also breaking and re-forming, in contrast with uncatalyzed capped SWNT at the same or even higher temperatures.[7] This can be explained by the extent over the entire tip structure of the Co electronic d orbitals close to the Fermi energy, which are coupled with the pentagon carbon π states, destabilizing selectively the pentagons. These cobalt states are found to completely fill the density of states near the Fermi energy, thus enhancing the chemical reacivity of the catalyzed nanotube tip.

During this QMD simulation, we observed that the Co atom is able to extract a carbon atom from the hemispherical cap and re-insert it within a more favorable topology, thus initiating a tip reconstruction. The re-incorporation event can also be viewed as the introduction of a new carbon atom into the catalytic closed-end termination of the tube. We thus performed static *ab initio* calculations at 0 K in order to estimate the corresponding incorporation barrier (Figure 2). In each calculation, the angle between the Co–extra C (in blue) bond and the axis, parallel to the nanotube axis and passing through the Co atom, is kept fixed to a precise value. The incorporation barrier is estimated to be 0.36 eV, which is weak and could explain the facility to incorporate the additional carbon necessary for growth.

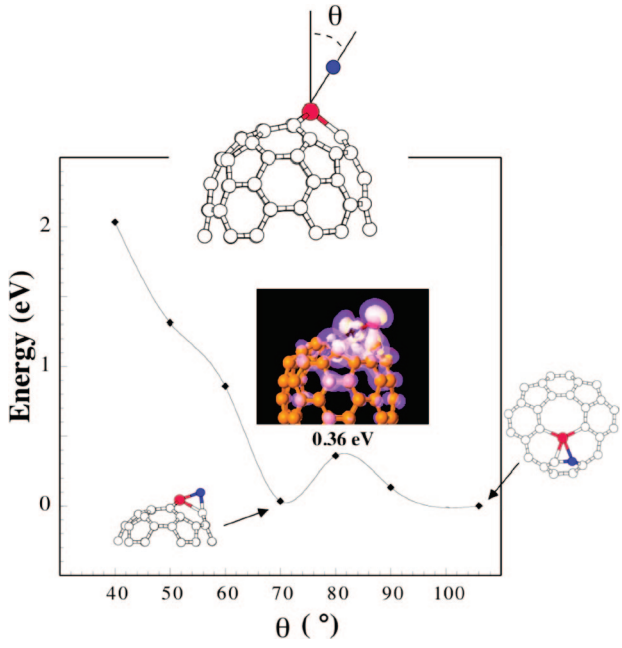

Figure 2. Static *ab initio* calculations of the incorporation barrier of an extra C atom into the Co-enriched nanotube tip. At the top of the 0.36 eV barrier, isovalue surfaces of local electron densities corresponding to electronic states localized on the carbon nanotube terminus, while incorporating the extra C atom. The electronic state is the HOMO state and illustrates the interaction between the π orbitals of the extra C atom and the d orbitals of the Co catalyst.

The electronic states of this atomic structure, at the top of the incorporation barrier, have also been computed. Some local densities of electronic states, filling the energy region close to the Fermi level (Figure 2), illustrate the interaction that occurs between the d-character orbitals of Co and the π orbitals of the extra C that is incorporated as well as with the surrounding carbon atoms. Although these orbitals are partially spread onto the entire tip, their prominent feature consists of the large-density lobes located on the metal atom and on neighboring carbon atoms. The Co atom acts as an electron donor and is also expected to play the role of a chemically active site, which should help in the incorporation of new carbon from the vapor phase.

To investigate this assumption, we also studied the impact of a single carbon atom on the catalyzed tube edge at ~2000 K. The carbon atom is initially projected along the nanotube axis with thermal velocity, starting at ~5 Å from the edge (see movie 2 in the electronic version of this article). During the QMD simulation, the Co atom clearly "stretches out" to capture the incoming C atom in order to maximize its coordination to carbon atoms. After some vibrations of this newly formed Co–C bond, a C–C bond from a neighboring pentagon reopens, capturing instantaneously the incoming atom in order to create a new hexagon, thus minimizing the energy of the tip apex structure, using a mechanism close to the one proposed in Figure 2. The breaking of C–C bonds in the neighboring region of the metal does provide active sites for the incorporation of incoming C atoms. Such a fast incorporation of carbon atoms from the vapor phase obtained in the catalytic growth of SWNTs should be contrasted with the *ab initio* simulation performed for SWNTs in the absence of metal transition.[7] A nanotube terminated by a perfect dome (hemi-fullerenes) containing six pentagons is sufficiently inert to resist any structural changes.[25]

The incorporation of a second carbon atom on the catalyzed edge at ~2000 K leads to an interesting tip topology, containing a Stone–Wales (SW) defect[26] (two pentagons and two heptagons coupled in pairs (5-7-7-5), see Figure 3). Such a defect can easily be transformed into four hexagons by a 90° rotation of a C–C bond about its center. However, this transformation is known to have an energy barrier of the order of 6–7 eV in a flat graphene sheet[27,28] and in C_{60}.[25,29] Our *ab initio* calculations show that, in the presence of the catalyst atom, the energy barrier is still 5.9 eV when the bond between the Co and the C dimer stays intact during the rotation (clockwise rotation, see Figure 3). However, this energy barrier is substantially reduced (3.25 eV) when the bond between the Co atom and the rotating dimer is broken during the transformation (anticlockwise rotation, see Figure 3). In the present case, the Co atom is found to bind loosely to the C dimer during the rotation, leading to an energy decrease for the SW transformation. This result suggests that the Co atom does play locally a key role in the reconstruction of the nanotube tip during the growth process.

In order to sample the "weakly characterized" carbon vapor phase, which may contain small clusters in addition to isolated atoms, a cluster containing two Co and five C has also been projected along the nanotube axis on the catalyzed tip apex. Again, the incoming fragment is found to be rapidly incorporated into the network of the nanotube tip, so that within less than 0.5 ps

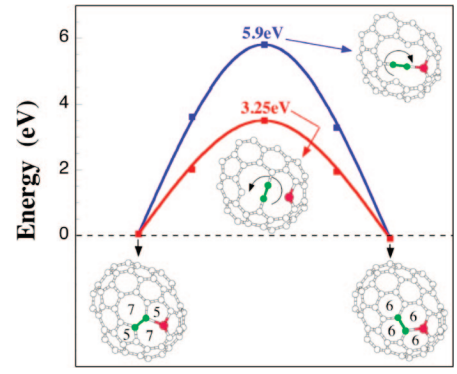

Figure 3. Transition energy barriers for a Stone–Wales defect into four hexagons by a simple 90° rotation of a C–C dimer (in green) included in the Co-riched nanotube tip. Energy is plotted *versus* a constrained reaction path. The usual barrier of ~6 eV is reduced to 3.25 eV when the rotating dimer (in green) involves the breaking of the C–Co bond (anti-clockwise rotation in the present topology).

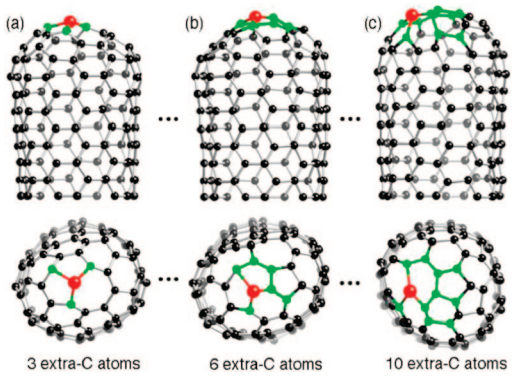

Figure 4. Incorporation of 3 (a), 6 (b), and 10 (c) extra C atoms on the catalytic closed end of a (6,6) armchair SWNT (side and top views). The Co atom is represented by a big red sphere, while the small green spheres correspond to the extra C atoms. In the equilibrium configurations, the Co–C bond lengths range from 1.9 to 2.1 Å.

of simulation, the incoming carbon atoms can no longer be distinguished from the atoms of the original nanotube. The system was further allowed to evolve for 4.5 ps to observe the evolution of the small Co cluster (three atoms) present on the apex of the tube. When several catalyst atoms aggregate at the tube edge, they do coalesce, suggesting the formation of the seed of a catalytic nanoparticle.

Ab initio MD calculations provide accurate descriptions of the chemical interactions, but those simulations are limited to small systems and short time scales. In order to investigate the incorporation of several extra C atoms on the catalyzed edge, *tight-binding* Monte Carlo (TB-MC) simulations have been performed (see Methods).

In order to study the incorporation of several extra C atoms into the SWNT, we performed TB-MC simulations at ~1000 K on the closing tube containing a single metallic atom, as depicted in Figure 1b. The extra C atoms were added, one by one, close to the tip, up to the point at which the global system could be considered to be at thermal equilibrium. Figure 4 illustrates some sequences in the growth of the nanotube where finally 10 extra C atoms have been added. The final structure is stable and corresponds to a length increase of roughly 1.6 Å. During the TB-MC simulation, we observed the same mechanism described previously, wherein the metal atom captures the incoming C atom to incorporate it into the structure. Moreover, the metal atom can also move laterally at the tip of the tube, as illustrated by its different positions in panels a and c of Figure 4. Finally, we also noted the insertion of an adatom into a heptagon defect, resulting in the creation of a pentagon–hexagon pair, leading to a more energetically favorable topology for the dome. Consequently, a succession of such easy incorporation of extra C atoms at different tip locations induces the extension of the tube and could be viewed as a tip growth mechanism at the atomic scale.

Although SWNTs have been produced by preformed catalytic particles,[12] which are attached to the tube end and thus closely correlated to the tube diameter (from 1 to 5 nm), these catalytic particles are not frequently observed at the tube end.[4] Nevertheless, several experimental works report on the presence of small metal particles attached on the walls of nanotube bundles,[30] but the catalytic effects of the metal in or on the side-wall are not discussed in the present paper.[31] Moreover, NMR experiments[32] have clearly demonstrated that ~0.5 wt % of each catalyst (Co, Ni), used to synthesize SWNTs, is found to remain in purified samples even after prolonged treatments in boiling concentrated HNO_3, suggesting that small metallic clusters or isolated atoms are incorporated in the graphitic structure of the nanotubes. Consequently, the presence of any remaining metal catalyst atoms at the nanotube tip (even in very small amounts) cannot be excluded. However, their presence, which is certainly not easy to establish experimentally, should really influence the field emission properties of these SWNTs and could probably be observed by looking at field emission patterns characterizing the tip composition and topology. Magnetic susceptibility measurements and magnetic STM could be used to investigate the presence of metal catalysts at the nanotube tip, as such experimental techniques are sensitive to tiny amounts of magnetic transition metals. At this stage, a better method for experimental characterization of the atomic structure of single-walled nanotube tips is required. The fact that pentagon–heptagon pair defects have been observed experimentally on several occasions is also an indication that this type of defect, catalyzed by the transition metal, plays a role in the growth of the structure. On some occasions, it may stay not repaired, perhaps because another active site has been formed on the top; the 5-7 pair defect stays incorporated and changes the chirality of the tube, as observed experimentally. At last, although SWNTs of different helicities have not been investigated here, the catalytic role played by the metal atom in substitution would be analogous in reconstructing a defect-free topology for a cap induced by a chiral nanotube.

In summary, our calculations suggest a possible microscopic mechanism for the catalytic growth of SWNTs using a closed-end mechanism. In the presence of a small amount of metal catalyst, the nanotube end geometry exhibits a high degree of chemical reactivity and accommodates several incoming carbon atoms, supporting a closed-end tip growth model. The latter may coexist with the usual root growth mechanism frequently proposed in the literature. Understanding the

growth mechanisms at the atomic level is crucial to designing procedures for controlling growth conditions to directly obtain more practical structures for nanotechnology.

METHODS

Quantum molecular dynamic (QMD) simulations are a powerful tool to explore dynamical effects such as growth, since they include both the influence of temperature on the motion of the atoms and the quantum mechanical description of the corresponding electronic system. In contrast to Born–Oppenheimer molecular dynamics, wherein the nuclear (ion) degrees of freedom are propagated using ionic forces which are calculated at each iteration by approximately solving the electronic problem with conventional matrix diagonalization methods, the Car–Parrinello method[33] used here explicitly introduces the electronic degrees of freedom as (fictitious) dynamical variables, writing an extended Lagrangian for the system which leads to a series of coupled equations of motion for both ions and electrons. In this way, an explicit electronic minimization at each iteration is not needed: after an initial standard electronic minimization, the fictitious dynamics of the electrons keep them on the electronic ground state corresponding to each new ionic configuration visited along the dynamics, thus yielding accurate ionic forces. In order to maintain this adiabaticity condition, it is necessary that the fictitious mass of the electrons is chosen small enough to avoid a significant energy transfer from the ionic to the electronic degrees of freedom. This small fictitious mass in turn requires that the equations of motion are integrated using a smaller time step than the ones (1–10 fs) commonly used in Born–Oppenheimer molecular dynamics.

In this approach,[33] the forces acting on the atoms are derived from the instantaneous electronic ground state, which is accurately described within density functional theory (DFT) in the local density approximation (LDA). The interaction between valence electrons and ionic cores is described using Troullier–Martins pseudopotentials for carbon and cobalt.[34] Periodic boundary conditions are adopted, keeping a minimum 7 Å distance in order to avoid interactions between repeated images. The electronic wavefunctions at the Γ-point of the supercell Brillouin zone are expanded into plane waves with a kinetic energy cutoff of 60 Ry. Within such a scheme, the calculated intraplanar lattice constant of graphite (2.46 Å), the C–C bond lengths in C_{60} (1.40 and 1.47 Å), and the lattice constant of hexagonal close-packed cobalt (2.49 Å) agree with experiment to within 1%. For each QMD run, the SWNT section is initially relaxed to its equilibrium geometry before being gradually heated to temperatures of 1500–2000 K by means of a Nosé thermostat.[35] The equations of motion are integrated using a time step of 0.7 fs.

In the *tight-binding* Monte Carlo (TB-MC) simulations, the interactions between metal and carbon atoms are treated within the semi-empirical *tight-binding* model, in which the total energy is a sum of local contributions, including a band structure term and an empirical repulsive term.[36] In this model, s,p electrons of the carbon and d electrons of the metal are taken into account. The local densities of electronic states are calculated using the recursion method.[37] To keep the model as simple and fast to compute as possible, we neglect the metal s electrons and calculate only the first four moments of the local densities of states. The local energy of each atom therefore depends only on the positions and chemical identities of its first and second neighbors, as defined by a cutoff distance set at 3.20 Å. Numerous tests were performed to check the reliability of the model: we obtain the same energy barrier for the continuous transformation of rhombohedral graphite to diamond as reported by Fahy *et al.*;[38] we retrieve the so-called clock reconstruction of the Ni(100) surface by simple relaxation of an adequate initial configuration,[39] and we could estimate a carbon solubility limit in crystalline Ni at 1500 K of ~6–8%, to be compared with the experimental value of 4%. Such an atomic interaction model has then been implemented in a Monte Carlo code, based on the Metropolis algorithm,[40] to study the relaxation of atomic structures at finite temperature and has recently been successfully tested on the dissolution and segregation of C in the presence of a Ni(111) surface.[18] In the present work, the TB-MC simulations are used in the canonical ensemble (with a fixed number of metal and C atoms) to study the incorporation of C atoms on the catalyzed edge, keeping fixed the neighboring bottom ring of carbons. The Monte Carlo computer simulation is organized as a series of macrosteps. Each macrostep randomly performs displacement moves for metallic and/or carbon atoms. Typical runs consist of 10^3 external Monte Carlo loops, each of them randomly performing 10^3 atomic displacements trials. This number of macrosteps is large enough to reach the equilibrium state.

Acknowledgment. The authors acknowledge scientific discussions with Xavier Blase, Roberto Car, Alessandro De Vita, and Gian-Marco Rignanese at the early stages of the present study and Christophe Bichara and François Ducastelle for the use of the TB-MC code. J.-C.C. is indebted to the National Fund for Scientific Research (FNRS) of Belgium for financial support. Parts of this work are also directly connected to the Belgian Program on Interuniversity Attraction Poles (PAI), to the ARC sponsored by the Communauté Française de Belgique, and to the NANOQUANTA and FAME European Networks of Excellence.

REFERENCES AND NOTES

1. Iijima, S. Helical Microtubules of Graphitic Carbon. *Nature* **1991**, *354*, 56–58.
2. Iijima, S.; Ichihashi, T. Single-Shell Carbon Nanotubes of 1-nm Diameter. *Nature* **1993**, *363*, 603–605.
3. Bethune, D. S.; Klang, C. H.; De Vries, M. S.; Gorman, G.; Savoy, R.; Vazquez, J.; Beyers, R. Cobalt-Catalysed Growth of Carbon Nanotubes with Single-Atomic-Layer Walls. *Nature* **1993**, *363*, 605–607.
4. Thess, A.; Lee, R.; Nikolaev, P.; Dai, H.; Petit, P.; Robert, J.; Xu, C.; Lee, Y. H.; Kim, S. G.; Rinzler, A. G.; Colbert, D. T.; Scuseria, G. E.; Tománek, D.; Fischer, J. E.; Smalley, R. E. Crystalline Ropes of Metallic Carbon Nanotubes. *Science* **1996**, *273*, 483–487.
5. Journet, C.; Maser, W. K.; Bernier, P.; Loiseau, A.; Lamy de la Chapelle, M.; Lefrant, S.; Deniard, P.; Lee, R.; Fischer, J. E. Large-Scale Production of Single-Walled Carbon Nanotubes by the Electric-Arc Technique. *Nature* **1997**, *388*, 756–758.
6. Gavillet, J.; Loiseau, A.; Journet, C.; Willaime, F.; Ducastelle, F.; Charlier, J.-C. Root-Growth Mechanism for Single-Wall Carbon Nanotubes. *Phys. Rev. Lett.* **2001**, *87*, 275504.
7. Charlier, J.-C.; De Vita, A.; Blase, X.; Car, R. Microscopic Growth Mechanisms for Carbon Nanotubes. *Science* **1997**, *275*, 647–649.
8. Kwon, Y.-K.; Lee, Y. H.; Kim, S.-G.; Jund, P.; Tománek, D.; Smalley, R. E. Morphology and Stability of Growing Multiwall Carbon Nanotubes. *Phys. Rev. Lett.* **1997**, *79*, 2065–2068.
9. Buongiorno Nardelli, M.; Brabec, C.; Maiti, A.; Roland, C.; Bernholc, J. Lip–Lip Interactions and the Growth of Multiwalled Carbon Nanotubes. *Phys. Rev. Lett.* **1998**, *80*, 313–316.
10. Saito, Y.; Okuda, M.; Fujimoto, N.; Yoshikawa, T.; Tomita, M.; Hayashi, T. Single-Wall Carbon Nanotubes Growing Radially from Ni Fine Particles Formed by Arc Evaporation. *Jpn. J. Appl. Phys.* **1994**, *33*, 526–529.
11. Saito, Y. Nanoparticles and Filled Nanocapsules. *Carbon* **1995**, *33*, 979–988.
12. Dai, H.; Rinzler, A. G.; Nikolaev, P.; Thess, A.; Colbert, D. T.; Smalley, R. E. Single-Wall Nanotubes Produced by Metal-Catalyzed Disproportionation of Carbon Monoxide. *Chem. Phys. Lett.* **1996**, *260*, 471–475.
13. Zheng, L. X.; O'Connell, M. J.; Doorn, S. K.; Liao, X. Z.; Zhao, Y. H.; Akhadov, E. A.; Hoffbauer, M. A.; Roop, B. J.; Jia, Q. X.; Dye, R. C.; Peterson, D. E.; Huang, S. M.; Liu, J.; Zhu, Y. T.

Ultralong Single-Wall Carbon Nanotubes. *Nat. Mater.* **2004**, *3*, 673–676.
14. Wu, J.; Dong, L.; Gutu, T.; Jones, J.; Jiao, J. Electron Microscopy Study of Carbon Nanotubes Synthesized by Plasma-Enhanced Chemical Vapor Deposition. *Microsc. Microanal.* **2006**, *12*, 652–653.
15. Helveg, S.; Lopez-Cartes, C.; Sehested, J.; Hansen, P. L.; Clausen, B. S.; Rostrup-Nielsen, J. R.; Abild-Pedersen, F.; Norskov, J. K. Atomic-Scale Imaging of Carbon Nanofibre Growth. *Nature* **2004**, *427*, 426–429.
16. Shibuta, Y.; Maruyama, S. Molecular Dynamics Simulation of Formation Process of Single-Walled Carbon Nanotubes by CCVD Method. *Chem. Phys. Lett.* **2003**, *382*, 381–386.
17. Ding, F.; Rosén, A.; Bolton, K. Molecular Dynamics Study of the Catalyst Particle Size Dependence on Carbon Nanotube Growth. *J. Chem. Phys.* **2004**, *121*, 2775–2779.
18. Amara, H.; Bichara, C.; Ducastelle, F. Formation of Carbon Nanostructures on Nickel Surfaces: A Tight-Binding Grand Canonical Monte Carlo Study. *Phys. Rev. B* **2006**, *73*, 113404.
19. Fan, X.; Buczko, R.; Puretzky, A. A.; Geohegan, D. B.; Howe, J. Y.; Pantelides, S. T.; Pennycook, S. J. Nucleation of Single-Walled Carbon Nanotubes. *Phys. Rev. Lett.* **2003**, *90*, 145501.
20. Raty, J.-Y.; Gygi, F.; Galli, G. Growth of Carbon Nanotubes on Metal Nanoparticles: A Microscopic Mechanism from *Ab Initio* Molecular Dynamics Simulations. *Phys. Rev. Lett.* **2005**, *95*, 096103.
21. Hofmann, S.; Csányi, G.; Ferrari, A. C.; Payne, M. C.; Robertson, J. Surface Diffusion: The Low Activation Energy Path for Nanotube Growth. *Phys. Rev. Lett.* **2005**, *95*, 036101.
22. Kiang, C.-H.; Goddard, W. A. Polyyne Ring Nucleus Growth Model for Single-Layer Carbon Nanotubes. *Phys. Rev. Lett.* **1996**, *76*, 2515–2518.
23. Lee, Y. H.; Kim, S. G.; Tománek, D. Catalytic Growth of Single-Wall Carbon Nanotubes: An Ab Initio Study. *Phys. Rev. Lett.* **1997**, *78*, 2393–2396.
24. Deng, W. Q.; Xu, X.; Goddard, W. A. A Two-Stage Mechanism of Bimetallic Catalyzed Growth of Single-Walled Carbon Nanotubes. *Nano Lett.* **2004**, *4*, 2331–2335.
25. Eggen, B. R.; Heggie, M. I.; Jungnickel, G.; Latham, C. D.; Jones, R.; Briddon, P. R. Autocatalysis During Fullerene Growth. *Science* **1996**, *272*, 87–90.
26. Stone, A. J.; Wales, D. J. Theoretical Studies of Icosahedral C_{60} and Some Related Species. *Chem. Phys. Lett.* **1986**, *128*, 501–503.
27. Crespi, V. H.; Benedick, L. X.; Cohen, M. L.; Louie, S. G. Prediction of a Pure-Carbon Planar Covalent Metal. *Phys. Rev. B* **1996**, *53*, R13303–R13305.
28. Buongornio-Nardelli, M.; Yakobson, B. I.; Bernholc, J. Mechanism of Strain Release in Carbon Nanotubes. *Phys. Rev. B* **1998**, *57*, R4277–R4280.
29. Ewels, C. P.; Heggie, M. I.; Briddon, P. R. Adatoms and Nanoengineering of Carbon. *Chem. Phys. Lett.* **2002**, *351*, 178–182.
30. Qin, L.-C.; Iijima, S. Structure and Formation of Raft-Like Bundles of Single-Walled Helical Carbon Nanotubes Produced by Laser Evaporation. *Chem. Phys. Lett.* **1997**, *269*, 65–71.
31. Andriotis, A. N.; Menon, M.; Froudakis, G. Catalytic Action of Ni Atoms in the Formation of Carbon Nanotubes: A Molecular Dynamics Study. *Phys. Rev. Lett.* **2000**, *85*, 3193–3196.
32. Dujardin, E.; Meny, C.; Panissod, P.; Kintzinger, J.-P.; Yao, N.; Ebbesen, T. W. Interstitial Metallic Residues in Purified Single Shell Carbon Nanotubes. *Solid State Commun.* **2000**, *114*, 543–546.
33. Car, R.; Parrinello, M. Unified Approach for Molecular Dynamics and Density-Functional Theory. *Phys. Rev. Lett.* **1985**, *55*, 2471–2474.
34. Troullier, N.; Martins, J.-L. Efficient Pseudopotentials for Plane-Wave Calculations. *Phys. Rev. B* **1991**, *43*, 1993–2006.
35. Nosé, S. Constant Temperature Molecular-Dynamics Methods. *Prog. Theor. Phys. Suppl.* **1991**, *103*, 1–46.
36. Amara, H. Ph.D. Thesis, Université Paris VI, 2005, (http://lem.onera.fr/Theses.html).
37. Haydock, R.; Heine, V.; Kelly, M. J. Electronic Structure Based on the Local Atomic Environment for Tight-Binding Bands. *J. Phys. C.: Solid State Phys.* **1972**, *5*, 2845–2858.
38. Fahy, S.; Louie, S. G.; Cohen, M. L. Theoretical Total-Energy Study of the Transformation of Graphite into Hexagonal Diamond. *Phys. Rev. B* **1987**, *35*, 7623–7626.
39. Klink, C.; Olesen, L.; Besenbacher, F.; Stensgaard, I.; Laegsgaard, E.; Lang, N. D. Interaction of C With Ni(100): Atom-Resolved Studies of the "Clock" Reconstruction. *Phys. Rev. Lett.* **1993**, *71*, 4350–4353.
40. Metropolis, N.; Rosenbluth, A. E.; Rosenbluth, M. N.; Teller, A. H.; Teller, E. Equations of State Calculations by Fast Computing Machines. *J. Chem. Phys.* **1953**, *21*, 1087–1092.